eNergetics 2025
DOI: https://doi.org/10.5281/zenodo.18621026

Original Scientific Article

HTL-Free 2D/3D Hybrid Perovskite Solar Cells: ETL Engineering and Simulation Insights

Walagedara Gamage Ayomi Pabasara[1], Galhenage Asha Sewvandi[2]

[1,2]Department of Materials Science and Engineering, University of Moratuwa, Katubedda, Sri Lanka
[1]Department of Engineering Technology, University of Ruhuna, Kamburupitiya, Sri Lanka

[1]ayomi@fot.ruh.ac.lk, [2]galhenagea@uom.lk

Abstract—**The commercialization of PSCs is hindered by instability under heat, moisture, and UV, which is mitigated by 2D/3D hybrids that combine the stability of 2D and the efficiency of 3D perovskites. Despite improvements in intrinsic material stability, conventional device architectures using hole transport layers (HTLs) still face challenges in long-term durability. In this study, we numerically investigate HTL-free carbon electrode-based 2D/3D hybrid PSCs, focusing on optimizing the 3D perovskite layer properties and evaluating different electron transport layer (ETL) materials. Devices using TiO_2, SnO_2, WS_2, and C_{60} as ETLs achieved maximum PCEs of 19.15%, 20.25%, 20.00%, and 22.26%, respectively, at optimal 3D layer thicknesses of 0.9 µm, 1.3 µm, 1.4 µm, and 1.2 µm, respectively. The performance of all devices was maximized at a bulk defect density of 10^{12} cm^{-3}. The results reveal that ETL has a significant impact on device performance in HTL-free 2D/3D hybrid PSCs. The study also highlights the critical role of the electrode work function, identifying 5.4 eV as the minimum threshold for efficient charge extraction in HTL-free 2D/3D hybrid PSCs.**

Keywords - HTL-free, carbon electrode, Perovskite solar cells, stability, SCAPS.

I. INTRODUCTION

Perovskite solar cells have garnered widespread attraction worldwide as a cutting-edge photovoltaic technology due to their higher efficiency and low-cost fabrication processes [1,2]. Over the past years, PSCs have marked rapid development due to intensive research efforts and technological advancements, leading to enhanced fundamental properties, including improved carrier mobility, light absorption, and reduced recombination losses. By 2024, the PCE has surpassed 26% revolutionizing the solar cell industry [3]. However, the PSCs still suffer from instability issues upon exposure to heat, moisture and UV radiation, which declines the performance and durability of the cell [4]. Several strategies have been suggested in the literature to enhance the stability of the PCSs, including encapsulations, additive engineering, and compositional tuning [5].

The two-dimensional form of perovskite materials demonstrates excellent environmental stability compared to their 3D counterparts [6-8]. Therefore, to leverage this advantage, 2D perovskites are incorporated into 3D perovskites to enhance stability, and the resultant architecture is known as 2D/3D mixed dimensional or hybrid PSCs [9]. This structure combines both high efficiency and superior charge transport characteristics of 3D perovskites with outstanding moisture and thermal stability of 2D perovskites, resulting in devices with both enhanced performance and long-term operational stability [10,11].

While these advances have overcome the intrinsic instability of 3D perovskites, the overall device stability can arise from the deterioration of the charge transport layers. The traditional

ISBN: 978-86-82602-07-1

device architecture of the PSCs comprises transparent conducting oxide/ETL/perovskite absorber layer/HTL/back contact electrode, which is often made from noble metals such as Au, Ag or Pt. The HTL materials are mostly made of Spiro-OMetAD which offers high efficiency; however, it is expensive and suffers from instability issues impending commercialization.

To overcome these challenges, researchers are making continuous research efforts to develop HTL-free PSCs. Carbon is used as HTL-free PSCs as a cost effective and promising alternative, serving both as a stable counter electrode and a substitution for traditional HTLs [12,13]. Carbon shows enhanced electrical conductivity, chemical stability and compatibility with large-scale fabrication techniques. However, these HTL-free devices demonstrate lower efficiency compared to the devices with HTLs and back electrodes with noble metals [14]. In particular, the photovoltaic performance of the HTL-free device heavily relies on the ETL materials as it is crucial in charge selectivity by electron extraction and blocking the holes [12]. Therefore, optimizing and selecting appropriate ETL materials with favorable energy level alignment and carrier mobility can substantially improve the device performance even the absence of HTL.

The efficiency of HTL-free PSCs based on 3D perovskites was relatively low, with early reports of around 6.6% [12,15]. Subsequent advances in compositional engineering and the application of new manufacturing methods significantly enhanced performance, leading to experimentally demonstrated efficiencies above 18% [16].

However, the feasibility of developing HTL-free, C electrode-based 2D/3D hybrid PSCs has not been systematically explored. This combination opens compelling pathways towards highly stable, cost-effective and efficient PSCs. In this research, the performance of HTL-free 2D/3D hybrid PSCs is investigated through numerical simulation, focusing on the effect of various ETL materials.

II. Device Design and Simulation

A. *Device Design*

The HTL-free carbon electrode 2D/3D hybrid PSCs were numerically simulated utilizing SCAPS 1D simulation software. Fig. 1 illustrates the device architecture of the proposed PSCs. Moreover, the AM 1.5 solar spectrum has been used for simulations. In the proposed device design, Methylammonium Lead Iodide ($MAPbI_3$) serves as the 3D perovskite material. As the 2D perovskite material, pentamethylenediamine (PeDA) based Dion Jacobson (DJ) perovskite materials (n=5) [$PeDAMA_4Pb_5I_{16}$] was selected, which has been proven to be more stable than monoamine-based Ruddlesden-Popper (RP) perovskites [17,18].

In this study, the device performance was optimized by employing four different ETL materials. C-electrode was selected as the back contact material. The thickness and defect densities of the 2D perovskite layer and the ETL layer were optimized, and those optimized parameters were adopted for simulation. Further, the effects of the thickness and defect density variation of the primary absorber layer were comprehensibly analyzed. The input parameters of each of the layers adopted from the published literature sources are mentioned in Table I. Electron and hole capture cross-section area were considered as 1×10-15 cms-1 while electron and hole thermal velocities were taken as 1×107 cm2 [12]. In this study, the SCAPS-1D simulations are conducted, assuming static ion positions, so that the impact of ion migration and respective hysteresis phenomena are not reflected.

B. *Materials Selection for ETL*

Four ETL materials were selected based on their stability and performance. TiO_2 is a commonly used ETL material in PSCs due to its optical transparency, chemical resistance, cost

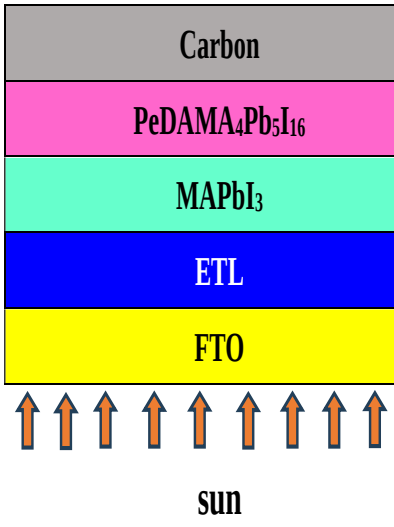

Figure 1. Proposed device architecture.

TABLE I. DETAILS OF BASIC SIMULATION PARAMETERS OF SOLAR CELL [12,17].

	$PeDAMA_4Pb_5I_{16}$ (2D)	**$MAPbI_3$ (3D)**	**TiO_2**	**SnO_2**	**WS_2**	**C_{60}**
Thickness (μm)	0.1	0.2-1.6	0.1	0.1	0.01	0.1
Band gap (eV)	1.6	1.55	3.26	4	2.38	1.7
Electron affinity (eV)	3.98	3.9	4.2	4.1	3.95	4
Dielectric permeability relative	25	3.2	38	12.5	13.6	10
VB effective density of state (states/cm^3/eV)	$7.5\cdot10^{17}$	$2.8\cdot10^{20}$	$2.2\cdot10^{17}$	$2.2\cdot10^{18}$	$1\cdot10^{18}$	$8\cdot10^{19}$
CB effective density of state (states/cm^3/eV)	$1.8\cdot10^{18}$	$3.9\cdot10^{20}$	$1.8\cdot10^{18}$	$1.8\cdot10^{19}$	$2.4\cdot10^{19}$	$8\cdot10^{19}$
Hole mobility (cm^2/Vs)	1.4	11.8	$2\cdot10^{4}$	100	100	$8\cdot10^{-2}$
Electron mobility (cm^2/Vs)	0.3	11.8	$1\cdot10^{3}$	25	100	$3.5\cdot10^{-6}$
Shallow uniform donor density (cm^{-3})	0	$1\cdot10^{9}$	$6\cdot10^{19}$	$5.9\cdot10^{19}$	$1\cdot10^{18}$	$1.0\cdot10^{21}$
Shallow uniform acceptor density (cm^{-3})	0	$1\cdot10^{9}$	0	0	0	0
Defect density	$2.4\cdot10^{14}$	$1\cdot10^{10}$-$1\cdot10^{16}$	$1\cdot10^{12}$	$1\cdot10^{12}$	$1\cdot10^{12}$	$1\cdot10^{12}$

effectiveness and ease of fabrication [19,20]. SnO_2 has shown excellent electron extraction, chemical stability, UV resistance and low temperature processing, making it a suitable candidate for ETL [21,22]. WS_2 is an abundant, nontoxic, low-cost, transparent material with enhanced carrier mobility and stability [23,24]. C_{60} is a widely used ETL material in HTL-free PSC which also exhibits excellent thermal stability for solar cell working temperatures range. Combined with Carbon electrode, it also demonstrates moisture resistance [25]. The favorable band alignment of ETL with the $MAPbI_3$ was also considered to ensure efficiency charge transportation. The initial performance of the devices is mentioned in Table II.

TABLE II. THE DEVICE PERFORMANCE BEFORE OPTIMIZATION.

ETL	**PCE (%)**	**V_{oc} (V)**	**J_{sc} (mA/cm^2)**	**FF (%)**
TiO_2	18.26	1.01	23.15	77.86
SnO_2	18.67	1.05	22.28	79.55
WS_2	18.52	1.08	22.76	75.21
C_{60}	21.12	1.09	25.95	75.00

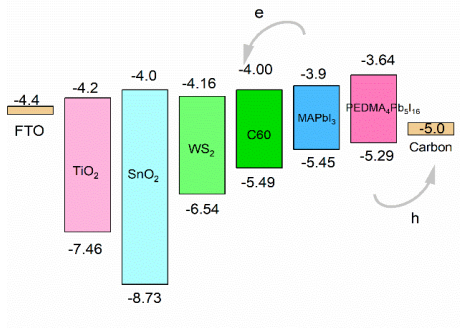

Figure 2. Energy band diagram.

III. Results and Discussion

A. *Energy Band Diagram*

Band alignment is vital in determining potential barriers that charge carriers must overcome to move between absorber layer and charge transportation materials. Optimal band alignment reduces these barriers, thereby increasing the carrier mobility and overall device performance. The band diagram of the PSCs in Fig. 2 illustrates the operating principle of the proposed solar cell with the HOMO (Highest Occupied Molecular Orbital) and LUMO (Lowest Unoccupied Molecular Orbital) energy of each layer. As per the diagram, photo-induced electrons are efficiently extracted towards the FTO due to the favorably aligned conduction bands of the 3D perovskite and selected ETLs.

B. *Impact of Primary Absorber Layer Thickness on the Device Performance*

The performance of 2D/3D hybrid PSCs is mainly driven by the thickness of the 3D perovskite layer as it directly influences the absorbed percentage of the solar irradiance by the perovskite material [26]. The 2D-PeDA perovskite layer primarily functions as a protective layer, and its contribution to light absorption is relatively low as the bandgap is relatively high [27].

Based on experimental findings, for this analysis, perovskite layer thickness varies from 0.3 µm to 1.6 µm with an increment of 0.1µm, keeping the other parameters constant. The behavior of PV characteristics against thickness variation is illustrated in Fig. 3. The optimum thicknesses are 0.9µm for TiO_2, 1.3 µm for SnO_2, 1.4µm for WS_2 and 1.2 µm for C_{60}. The corresponding PCEs achieved were 18.92%, 20.06%, 19.77%, and 22.01%, respectively.

The effect of thickness on performance can be linked to thickness-dependent absorption characteristics of the primary absorber layer. In the relatively lower thicknesses, the absorption in

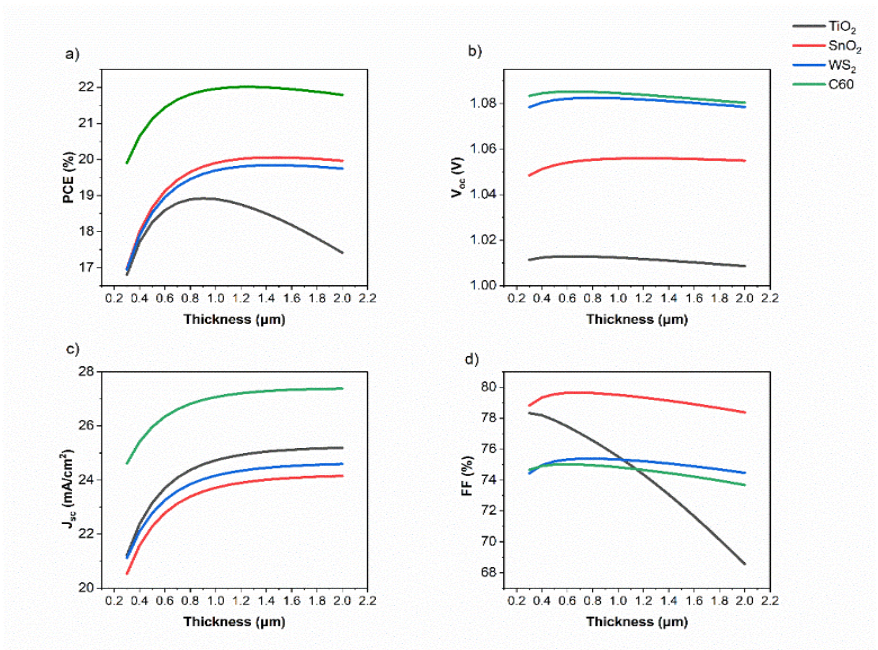

Figure 3. Effect of 3D layer thickness on the performance of PSCs with different ETLS a) PCE b) Voc c) Jsc d) FF.

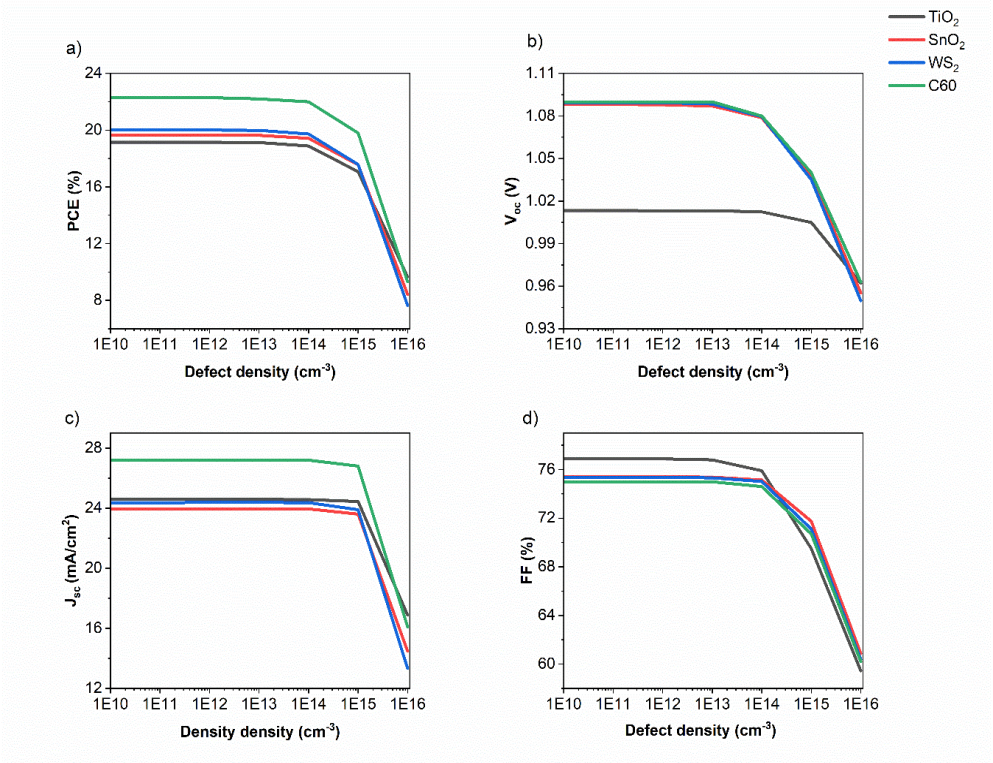

Figure 4. Effect of 3D layer defect density on the performance of PSCs with different ETLs a) PCE b) Voc c) Jsc d) FF.

the longer wavelength is limited, resulting in limited electron-hole pair generation. Increasing the thickness enhances the absorption of longer wavelengths, leading to improved electron-hole pair generation. However, when thickness surpasses a critical value, even a greater portion of the solar spectrum can be absorbed, and the generated charge carriers must travel long distances to reach their respective electrodes, increasing the likelihood of carrier recombination. Subsequently, the PCE of the device degrades after the thickness exceeds a critical threshold. V_{oc} and FF decrease when the absorber layer thickness rises. This is mainly caused by the enhanced carrier recombination and series resistance due to thickness increase. The thicker absorber layer introduces more series resistance, leading to voltage drop during current flow and hindering the efficient charge collection, thereby reducing the V_{oc}. The drop of V_{oc} lowers the maximum output power and consequently decreases FF [2]. The highest PCE is achieved by the device with C_{60}.

C. Impact of Primary Absorber Layer Defect Density on the Device Performance

3D-$MAPbI_3$ layer acts as the main light harvesting layer, playing a key role in deciding the performance of the device. Perovskite including vacancies, interstitials, impurities, Schottky, and Frankel defects [28]. The impact of the deep and shallow defects on the performance was investigated materials contain different intrinsic defects, varying the defect density in the range of $1 \cdot 10^{10}$ cm^{-3} to $1 \cdot 10^{16}$ $cm^{-3,}$ keeping the other parameters constant. As per Fig. 4, all photovoltaic performance remains stable up to a critical threshold defect density value. Once the defect density exceeds this threshold limit, all photovoltaic parameters gradually decline. This decline can be attributed to increased recombination losses, which become more prominent at higher defect density values. Consequently, the carrier diffusion length of charges declines, leading to a reduction in carrier lifetime [29]. At the critical defect density value of $1 \cdot 10^{12}$ cm^{-3}, the TiO_2, SnO_2, $WS_{2,}$ and C_{60} ETL-based devices show a maximum PCE of 19.15%, 19.63%, 20.01% and 22.26%, respectively.

E. The Optimized Device Performance

The recorded optimum performance of the devices and corresponding IV characteristic curves are mentioned in Table III and Fig. 5, respectively.

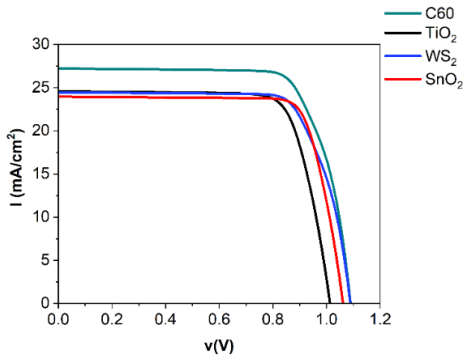

Figure 5. IV characteristics of the proposed devices based on different ETLs.

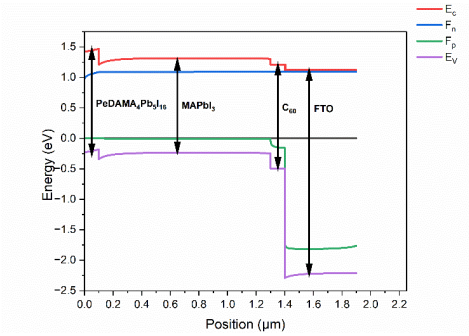

Figure 6. Band structure of the C60 ETL-based PSC with highest performances (Ec- conduction band minimum, Ev- valance band maximum, Fn- Electron quasi-fermi level, Fp- Hole quasi-fermi level).

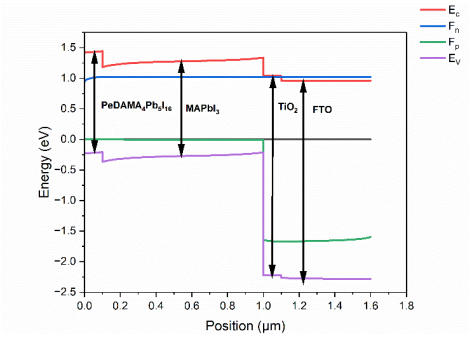

Figure 7. Band structure of the TiO2 ETL-based PSC with lowest performances (Ec- conduction band minimum, Ev- valance band maximum, Fn- Electron quasi-fermi level, Fp- Hole quasi-fermi level).

TABLE III. THE DEVICE PERFORMANCE AFTER OPTIMIZATION.

ETL	PCE (%)	V_{oc} (V)	J_{sc} (mA/cm^2)	FF (%)
TiO_2	19.15	1.01	24.58	71.84
SnO_2	20.25	1.06	23.96	79.61
WS_2	20.00	1.09	24.37	75.36
C_{60}	22.26	1.09	27.21	74.34

The reasons for the performance differences can be explained by comprehensively investigating the energy band diagrams. The corresponding energy band diagrams of the best performing and the lowest performing devices are illustrated in Figs. 6 and 7, respectively. As the devices have utilized different ETLs, their energy band alignment with the $MAPbI_3$ perovskite absorber is the main reason for performance disparity. The energy band diagrams exhibit that the conduction band minimum (E_c) of C_{60} is better aligned with the E_c of $MAPbI_3$ compared to that of TiO_2. In the C_{60}-based devices, the conduction band offset (CBO) between C_{60} and $MAPbI_3$ layer is smaller than TiO_2-based devices, making a smooth transition for electrons from the 3D perovskite layer to the ETL. This favorable alignment minimizes the energy barrier for electron extraction and improves charge collection efficiency, reducing the likelihood of interfacial recombination. As a result of that, the C_{60}-based device achieves a higher open-circuit PCE and V_{oc}. In contrast, the TiO_2-based device has a larger CBO between TiO_2 and $MAPbI_3$ layer, creating a larger energy barrier for electron extraction. This barrier increases the carrier concentration at the interface and, thus, recombination rates and energy losses. As a result of that, the TiO_2-based device shows comparatively poor performance. In experimental studies, a carbon-based PSC using FTO/c-TiO_2/m-TiO_2/3D-$FAPbI_3$ with Octylam-ammonium iodide based 2D perovskite layer achieved a PCE of 18.25% which is highly consistent with the results of our simulations, thereby validating the study [16].

The device performances can be further enhanced by adjusting the recombination rates, series and shunt resistance, and acceptor and donor concentrations.

F. Impact of the Work Function of the Back Contact on the Device Performance

The impact of the metalwork function of the back contact electrode on the device performance was examined. It's a primary property of the metal that impacts how it interacts with materials

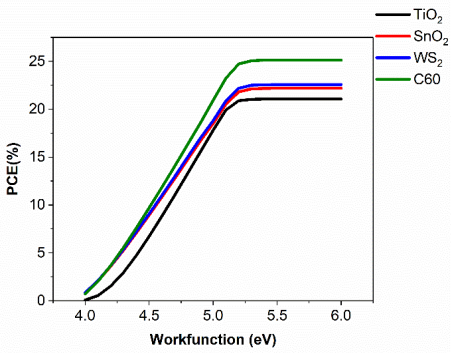

Figure 8. Effect of the metalwork function on PCE of the PSCs with different ETLs.

such as semiconductors. As the work function of the back-contact electrode increases, it ensures more favorable energy level alignment with the perovskite layer, ensuring better hole extraction and minimizing recombination losses, which leads to a significant rise in PCE until it saturates at optimal alignment as per Fig. 8 [30]. In conventional PSCs, noble metals such as Au, Ag, and Pt are widely used as back contact materials. Due to their high cost, alternative materials such as Cu, Al, and C are widely investigated to replace the noble metals. For maximum performance of the device, the back contact electrode should have a minimum 5.4 eV work function as shown in Fig. 8. The work function of the C electrode can be enhanced through doping, which is a cost-effective option, unlike noble metals [31]. Doping optimizes energy level alignment, reducing defects, and blocking environmental factors. Doping can fine-tune the work function for better charge extraction, while interface engineering can passivate trap states, prevent direct contact with degrading substances, and improve overall mechanical and chemical stability, leading to higher efficiency and longevity.

IV. Conclusion

HTL-free carbon electrode based 2D/3D hybrid PSCs have been numerically simulated, focusing on optimizing the 3D perovskite layer thickness and defect density to enhance performance. At the defect density of 10^{12} cm^{-3}, all devices exhibited maximum performance.

For different ETL materials, the optimum 3D perovskite layer thicknesses were reported to be: 0.9 µm for TiO_2, 1.3 µm for SnO_2, 1.4 µm for WS_2, and 1.2 µm for C_{60}. The maximum PCEs achieved were 19.15%, 20.25%, 20.00%, and 22.26%, respectively. The C_{60} based PSC outperform with V_{oc} of 1.09V, J_{sc} of 27.21 mA/cm^2 and FF of 74.34%. Furthermore, the impact of the metal work function on device performance was investigated, revealing that a minimum of 5.4 eV is required for optimal charge extraction. Carbon electrodes can be a cost-effective option, achieving similar performance if appropriate doping strategies are used to improve their work function.

References

[1] Leung, T. L., Ahmad, I., Syed, A. A., Ng, A. M. C., Popović, J., & Djurišić, A. B. (2022). Stability of 2D and quasi-2D perovskite materials and devices. *Communications Materials*, 3(1), 1–10.

[2] Gamage Ayomi Pabasara, W., & Asha Sewvandi, G. (2025, January 20). Numerical simulation and optimization of stable $CH_3NH_3PbI_3$-based 2D/3D mixed dimensional perovskite solar cell. In *Proceedings of the 10th Virtual International Conference on Science, Technology and Management in Energy (eNergetics 2024)*, Virtual.

[3] Green, M. A. A., et al. (2025). Solar cell efficiency tables (version 65). *Progress in Photovoltaics: Research and Applications*, 33(1), 3–15.

[4] Fan, Y., Meng, H., Wang, L., & Pang, S. (2019). Review of stability enhancement for formamidinium-based perovskites. *Solar RRL*, 3(9), 1–18.

[5] Wang, R., Mujahid, M., Duan, Y., Wang, Z. K., Xue, J., & Yang, Y. (2019). A review of perovskite solar cell stability. *Advanced Functional Materials*, 29(47), 1–25.

[6] Choi, H.-S. S., & Kim, H.-S. S. (2020). 3D/2D bilayer perovskite solar cells with enhanced stability and performance. *Materials*, 13(17).

[7] Li, D., Xing, Z., Meng, X., Hu, X., Hu, T., & Chen, Y. (2023). Selection of functional spacer cations for efficient 2D/3D perovskite solar cells. *CCS Chemistry*, 5(4), 71–801.

[8] Ye, X., et al. (2022). Organic spacer engineering in 2D/3D hybrid perovskites for efficient and stable solar cells. *New Journal of Chemistry*, 46(6), 2837–2845.

[9] Li, X., et al. (2023). Mixed perovskites (2D/3D)-based solar cells: A review on crystallization and surface modification for enhanced efficiency and stability. *Advanced Composites and Hybrid Materials*, *6*(3), 1–27.

[10] Sutanto, A. A., et al. (2020). Dynamical evolution of the 2D/3D interface: A hidden driver behind perovskite solar cell instability. *Journal of Materials Chemistry A*, 8(5), 2343–2348

[11] Ji, C., et al. (2021). Interface engineering of 2D/3D perovskite heterojunction improves photovoltaic efficiency and stability. *Solar RRL*, 5(5), 1–9.

[12] Ijaz, S., et al. (2024). A numerical approach to optimize the performance of HTL-free carbon electrode-based perovskite solar cells using organic ETLs. *Heliyon*, 10(7), e29091.

[13] Danladi, E., et al. (2023). Impact of hole transport material on perovskite solar cells with different metal

electrode: A SCAPS-1D simulation insight. *Heliyon*, 9(6), 16838.

[14] Chen, R., et al. (2020). Carbon-based HTL-free modular perovskite solar cells with improved contact at perovskite/carbon interfaces. *Journal of Materials Chemistry C*, 8(27), 9262–9270.

[15] Ku, Z., Rong, Y., Xu, M., Liu, T., & Han, H. (2013). Fully printable processed mesoscopic CH3NH3PbI3/TiO2 heterojunction solar cells with carbon counter electrode. *Scientific Report*s, 3.

[16] Salma, Z., et al. (2022). Employing 2D-perovskite as an electron blocking layer in highly efficient (18.5%) perovskite solar cells with printable low-temperature carbon electrode. *Advanced Energy*, 12(21).

[17] Mohammed, M. K. A. A., et al. (2023). Harnessing the potential of Dion–Jacobson perovskite solar cells: Insights from SCAPS simulation techniques. *Journal* of *Alloys and Compounds*, 963, 171246.

[18] Chaurasia, S., et al. (2024). Highly efficient and stable Dion–Jacobson (DJ) 2D–3D perovskite solar cells with 26% conversion efficiency: A SCAPS-1D study. *Journal of Physics and Chemistry of Solids*, 191, 112038.

[19] Bulowski, W., et al. (2024). Optimization of the ETL titanium dioxide layer for inorganic perovskite solar cells. *Journal of Materials Science*, 59(17), 7283–7298.

[20] Mohammadi, S., Akbari Nia, S., & Abbaszadeh, D. (2024). Reduction of recombination at the interface of perovskite and electron transport layer with graded Pt quantum dot doping in ambient air-processed perovskite solar cell. *Scientific Reports*, 14(1), 1–12.

[21] Kim, J., Kim, K. S., & Myung, C. W. (2020). Efficient electron extraction of SnO2 electron transport layer for lead halide perovskite solar cell. *npj Computational Materials*, 6(1), 1–8.

[22] Mbilo, M., et al. (2024). Highly efficient and stable organic solar cells with SnO2 electron transport layer enabled by UV-curing acrylate oligomers. *Journal of Energy Chemistry*, 92, 124–131.

[23] Bin Rafiq, M. K. S., et al. (2020). WS2: A new window layer material for solar cell application. *Scientific Reports*, 10(1), 1–11.

[24] Malek, N. A. A., et al. (2020). Enhanced charge transfer in atom-thick 2H–WS2 nanosheets' electron transport layers of perovskite solar cells. *Solar RRL*, 4(10), 1–11.

[25] AlZoubi, T., et al. (2024). Advanced optoelectronic modeling and optimization of HTL-free FASnI3/C60 perovskite solar cell architecture for superior performance. *Nanomaterials*, 14(12).

[26] Chakrabartty, J., Islam, M. A., & Reza, S. (2021). Performance analysis of highly efficient 2D/3D bilayer inverted perovskite solar cells. *Solar Energy, 230*, 195–207

[27] Li, M.-H., et al. (2018). Highly efficient 2D/3D hybrid perovskite solar cells via low-pressure vapor-assisted solution process. *Advanced Materials*, 30(30), e1801401.

[28] Jayawardane, S. T., Akmal, M., Hu, D., Kumara, P., & Abeygunawardhana, W. (2024). Simulation-based performance analysis of lead-free bismuth perovskite solar cells: A comparative study of Cs3Bi2I9 and (CH3NH3)3Bi2I9-based perovskite solar cells. A*dvanced Theory and Simulations*, 7(7), 2400206

[29] Gholami-Milani, A., Ahmadi-Kandjani, S., Olyaeefar, B., & Kermani, M. H. (2023). Performance analyses of highly efficient inverted all-perovskite bilayer solar cell. *Scientific Reports, 13*(1), 1–15.

[30] Rayhan, A., Khan, M. A., & Islam, R. (2024). Enhancing CsSn0.5Ge0.5I3 Perovskite Solar Cell Performance via Cu2O Hole Transport Layer Integration. *International Journal of Photoenergy, 17*.

[31] Don, M. F., Ekanayake, P., Jennings, J. R., Nakajima, H., Kumar, U. D., & Lim, C. M. (2023). Influence of metal salts (Al, Ca, and Mg) on the work function and hole extraction at carbon counter electrodes in perovskite solar cells. *Heliyon*, 9(7), e17748.